

## PREDICTION OF FORMATION OF RECURVED SAND SPIT USING BG MODEL

Masumi Serizawa<sup>1</sup>, Takaaki Uda<sup>2</sup> and Shiho Miyahara<sup>1</sup>

The morphological features of recurved sand spits were studied by selecting recurved sand spits in Namibia, Sandy Hook on the US east coast, and Graswarder spit in Germany. The elongation of a recurved spit was predicted using the BG model (a model for predicting three-dimensional beach changes based on Bagnold's concept). A recurved spit was formed in Case 1 when waves were incident at angles of  $45^\circ$  and  $-30^\circ$  with a duration ratio of 0.85:0.15. The width of the recurved sand spit in Case 1 increased with the elongation of sand spit, and the overall shape became similar to the expanded bird wing, which well explains the configuration of a recurved sand spit formed in Namibia. In Case 2 when waves were obliquely incident at angles of  $45^\circ$  and  $-45^\circ$  with the same duration ratio as in Case 1, a sand spit extended straight, which well resembles Graswarder spit in Germany.

*Keywords: recurved sand spit; formative mechanism; BG model; Graswarder spit; Sandy Hook; Namibia*

### INTRODUCTION

When waves are obliquely incident at a large angle over  $45^\circ$  relative to the direction normal to the mean shoreline, a small perturbation on the shoreline may develop owing to the instability mechanism (high-angle waves), resulting in the formation of sand spits along the shoreline (Ashton et al. 2001). When two sets of waves arrive from different directions, however, the sand spit is recurved (Bird 2008). In a recurved spit, the previous shoreline often intersects at an acute angle with the overall elongation direction of the sand spit. The formation of this type of recurved spit was schematically explained by Zenkovich (1967), as shown in Fig. 1. When waves are obliquely incident to the shoreline from directions A and B, longshore sand transport toward the tip of the sand spit arises, resulting in the extension of the sand spit owing to the additional deposition of littoral sand. However, a significantly recurved spit may be formed if additional waves arrive from direction C opposing direction A. There have been few studies on the prediction of the elongation of a recurved sand spit when waves are incident from two directions. Uda et al. (2016) developed a model for predicting the formation of a cusped foreland when waves are incident from two opposing directions using the BG model (a model for predicting three-dimensional beach changes based on Bagnold's concept) (Serizawa et al. 2006). In this study, the elongation of a recurved spit was predicted using the same model as that employed in predicting the development of a cusped foreland when waves were incident from two opposing directions. First, the morphological features of recurved sand spits were studied, taking recurved sand spits in Namibia, Sandy Hook on the US east coast, and Graswarder spit in Germany as examples, and then a numerical simulation was carried out.

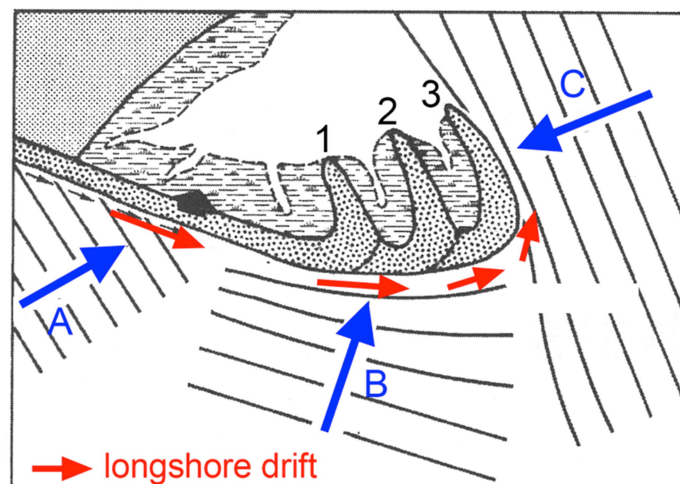


Figure 1. Schematic diagram of development of a recurved sand spit (Zenkovich 1967).

<sup>1</sup> Coastal Engineering Laboratory Co., Ltd., 1-22-301 Wakaba, Shinjuku, Tokyo 160-0011, Japan

<sup>2</sup> Public Works Research Center, 1-6-4 Taito, Taito, Tokyo 110-0016, Japan

## EXAMPLES OF RECURVED SAND SPITS

### Recurved Spit in Namibia in Southern Africa

A recurved sand spit with an overall shoreline that extends straight but is recurved at the tip can be observed on the coastline in Namibia facing the South Atlantic Ocean. Figure 2 shows a satellite image of sand spits with a regular shape formed along the coastline. Four sand spits can be observed in the rectangular area of 126 km width and 277 km length in the E-W and S-N directions, respectively. Figure 3 shows an enlarged satellite image of the rectangular area shown in Fig. 2, in which the horizontal axis was rotated clockwise by 90°. In Fig. 3, points A, B, C, and D are the locations where the shoreline protrudes furthest offshore near the tip of the sand spit, and the sand spits are also called A, B, C, and D. The intervals between these sand spits are 62, 68, and 43 km, with an average interval of 58 km. Sand spit B is the largest, and the sand spits become smaller and more slender north of sand spit B. An enlarged satellite image of the rectangular area (sand spit C) in Fig. 3 is shown in Fig. 4, with the shoreline configuration of sand spit C measured on December 31, 1984. The shoreline of sand spit C extends straight in the direction of N20°W from the south end, and the shoreline gradually rotates clockwise, forming a recurved spit at the north end. Many ridges that obliquely intersect with the present shoreline, which was formed by the continuous long-term deposition of sand, can be observed in the northern part of the sand spit. Comparing the shapes of the shorelines of the sand spit in 1984 and 2016, the southern part of the sand spit is almost identical, but sand has been deposited at the north end of the sand spit, resulting in its further extension by 750 m between 1984 and 2016. In addition, the elongating tip is smoothly connected to the shoreline of the overall sand spit, although the sand spit is recurved.

British Maritime Technology (1986) reported world ocean wave statistics in 104 subareas of the world's oceans, which were determined by direct wave observation and the wave hindcasting method. In this report, wave statistics offshore of Namibia can be found in subarea No. 85. Because the coastline of Namibia runs in the S-N direction, as shown in Fig. 2, waves incident from the east can be neglected. Thus, the probability of occurrence of waves incident from other directions becomes 2.37% (N), 5.64% (NW), 9.30% (W), 12.99% (SW), and 35.91% (S). The probability of occurrence of southerly waves is thus 48.9%, which is much greater than 8.01% for northerly waves, and the most predominant wave direction is south, which is approximately parallel to the overall shoreline, implying oblique wave incidence at a sufficiently large angle to cause shoreline instability (Ashton et al. 2001). Because of this, the sand spit extended northward, but waves from opposing directions to the predominant wave direction may be incident to the sand spit.

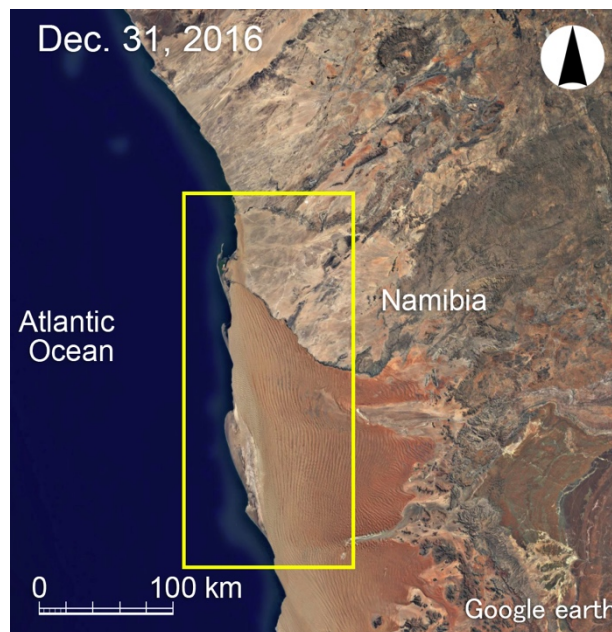


Figure 2. Satellite image of sand spits formed along Namibia coast.

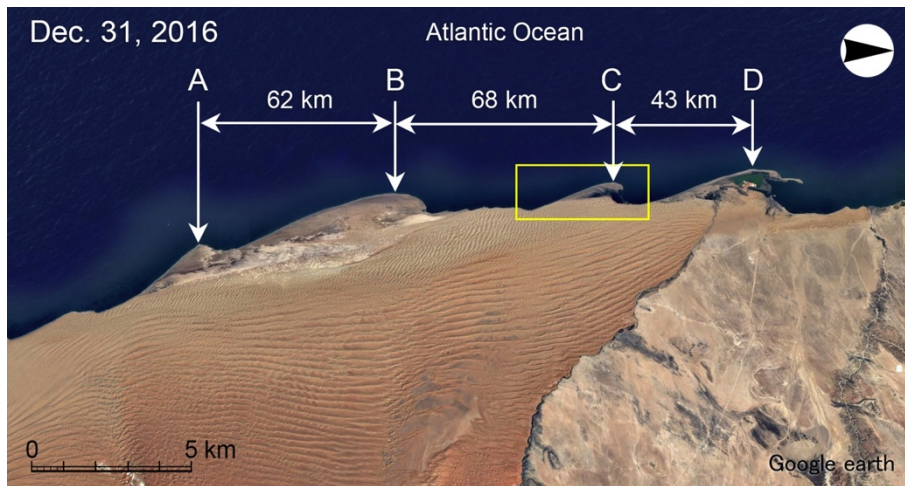


Figure 3. Enlarged satellite image of the rectangular area in Fig. 2.



Figure 4. Satellite images of sand spit C on December 31, 1984 and December 31, 2016.

**Sandy Hook in US East Coast**

At the north end of New Jersey on the US east coast, a recurved sand spit, Sandy Hook, with approximately 10 km length extends, separating the Atlantic Ocean and the Lower Bay. Figures 5 and 6 show a satellite image of a wide area surrounding Sandy Hook and an enlarged satellite image of the rectangular area in Fig. 5, respectively. Long Island is located north of the sand spit, a stable shoreline has formed at point P upcoast of a jetty of the inlet at the west end of Jones Beach State Park in Fig. 5, and the direction normal to the shoreline at point P is  $N21^{\circ}W$ . The predominant wave direction in this area is assumed to be approximately equal to this direction. In contrast, the direction normal to the shoreline at point Q taken at the base of Sandy Hook is  $N84^{\circ}E$ , with a large angle of  $75^{\circ}$  relative to the

direction of the mean shoreline. This oblique wave incidence at an angle over  $75^\circ$  is the reason for the northward elongation of Sandy Hook.

The incidence of westerly and northerly waves can be neglected in this area, because Sandy Hook is located at the west end of the Atlantic Ocean and close to Long Island, which shelters Sandy Hook against northerly waves, as shown in Fig. 5. From the wave statistics offshore of Sandy Hook in subarea No. 15 (British Maritime Technology 1986), the occurrence of waves except for those in the above directions becomes 6.67% (E), 7.11% (SE), and 17.0% (S). The prevailing wave direction is from the south, the same direction as the mean shoreline of Sandy Hook, and because of this, Sandy Hook elongated northward. Although the shoreline along the Atlantic Ocean almost smoothly extends except at the tip of the sand spit in Fig. 6, there are four protrusions on the bay side while preserving the geomorphological characteristics as a recurved sand spit. The overall shape is similar to that of the recurved sand spit in Namibia shown in Fig. 4.

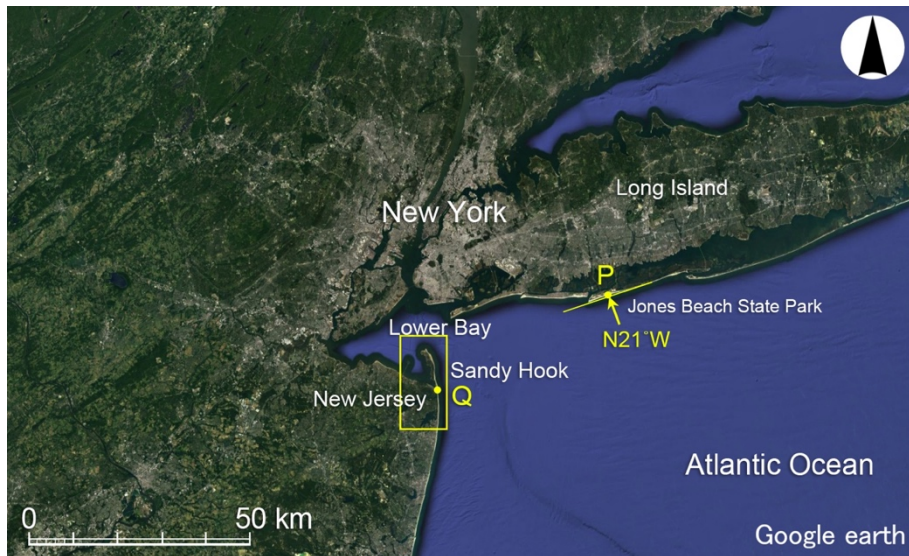


Figure 5. Location of Sandy Hook on US east coast.

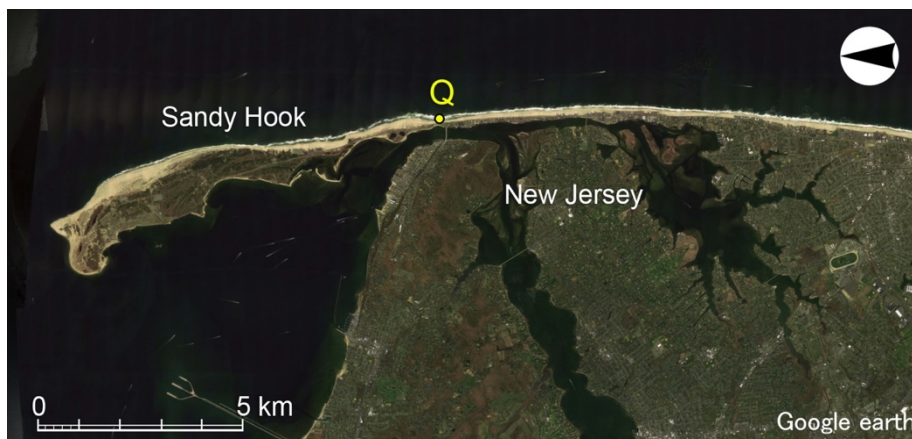


Figure 6. Satellite image of Sandy Hook.

#### Graswarder Spit in Germany

A compound spit comprising many superimposed recurved sand spits, where the elongating direction of the shoreline at the tip of the sand spit is significantly different from the overall direction of the sand spit can be seen in Germany. This spit significantly differs from the two examples discussed above. Figure 7 shows this sand spit, Graswarder spit, formed behind Fehmarn Island facing Fehmarn Belt in Germany at the entrance of the Baltic Sea (Bird 2010). Figure 8 shows an enlarged satellite

image of the rectangular area in Fig. 7. In addition, Fig. 9 shows satellite images of the rectangular area in Fig. 8 taken on December 31, 2007 and July 1, 2015. Although the sand spit extends eastward, many recurved spits are superimposed in the eastern part of the spit. The shoreline of each recurved spit intersects at an acute angle to the direction of the extension of overall sand spit, and 20 recurved spits can be seen. The development pattern of this sand spit differs from those of the spits in Namibia and Sandy Hook. The sand spit with many ridges extended by eastward longshore sand transport, and the barrier island has grown eastward for about 3,000 years with the addition of successive recurves (Bird 2010). The interval between the formation of successive recurved sand spits was estimated to be 150 years. Figure 10 shows an enlarged satellite image of the rectangular area shown in Fig. 9, where the shoreline in 2007 is superimposed on the satellite image in 2015. It can be seen that the tip of the sand spit extended southeastward by 120 m between Dec. 31, 2007 and July 1, 2015, and the elongation direction of the sand spit differs by  $90^\circ$  from the overall elongation direction of the recurved spit, implying that wave incidence from SE is necessary for many recurved spits to be formed.

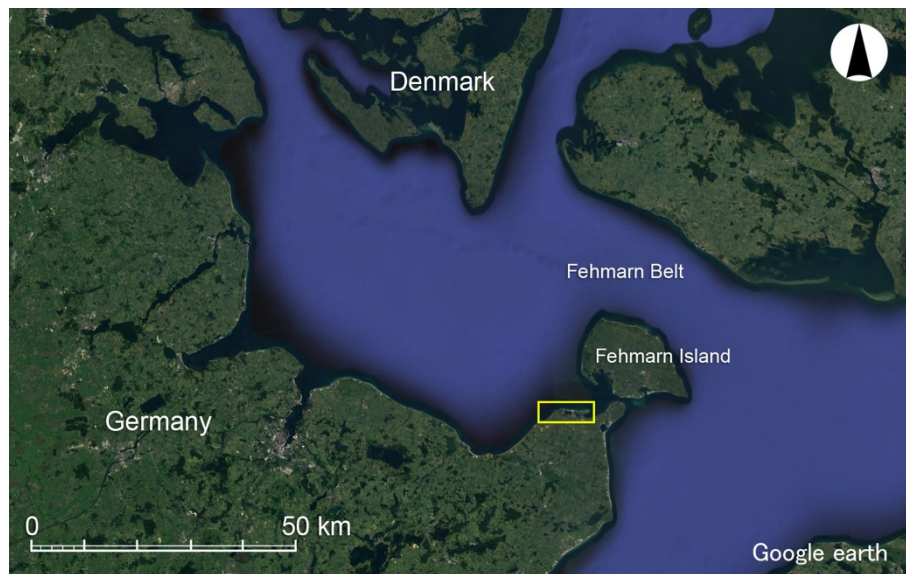


Figure 7. Location of Graswarder spit formed behind Fehmarn Island facing Fehmarn Belt in Germany.



Figure 8. Enlarged satellite image of Graswarder spit.



Figure 9. Change in Graswarder spit between 2007 and 2015.

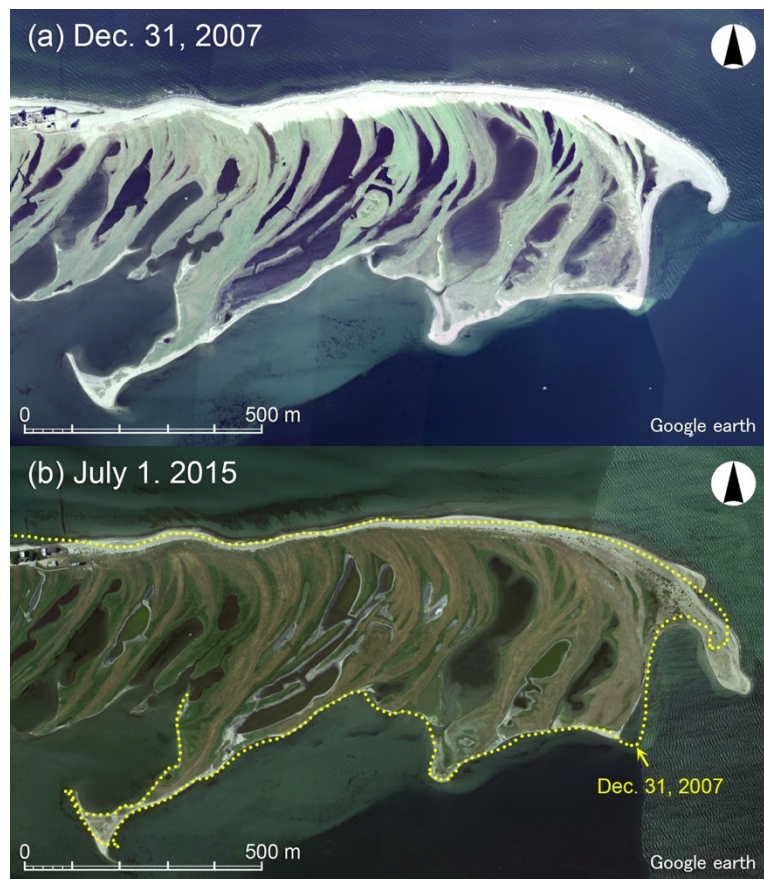


Figure 10. Satellite images and shoreline change at tip of Graswarder spit.

**NUMERICAL MODEL (BG MODEL)**

Numerical simulation of the formation of a recurved spit was carried out using the BG model (Uda et al. 2014; 2016). which is equal to the Type 4 BG model in Uda et al. (2018). We use the Cartesian coordinates  $(x, y)$  and consider the elevation at point  $Z(x, y, t)$  as a variable to be solved, where  $t$  is time. The beach changes were assumed to occur between the depth of closure  $h_c$  and the berm height  $h_R$ . The fundamental equation is given as follows.

$$\bar{q} = C_0 \frac{P}{\tan \beta_c} \left\{ \begin{array}{l} K_n (\tan \beta_c \bar{e}_w - |\cos \alpha| \bar{\nabla} Z) \\ + \left\{ (K_s - K_n) \sin \alpha - \frac{K_2}{\tan \bar{\beta}} \frac{\partial H}{\partial s} \right\} \tan \beta \bar{e}_s \end{array} \right\} \quad (1)$$

$$(-h_c \leq Z \leq h_R)$$

Here,  $\bar{q} = (q_x, q_y)$  is the net sand transport flux,  $n$  and  $s$  are the local coordinates taken along the directions normal (shoreward) and parallel to the contour lines, respectively,  $\bar{\nabla} Z = (\partial Z / \partial x, \partial Z / \partial y)$  is the slope vector,  $\bar{e}_w$  is the unit vector of the wave direction,  $\bar{e}_s$  is the unit vector parallel to the contour lines,  $\alpha$  is the angle between the wave direction and the direction normal to the contour lines,  $\tan \beta = |\bar{\nabla} Z|$  is the seabed slope,  $\tan \beta_c$  is the equilibrium slope, and  $\tan \beta \bar{e}_s = (-\partial Z / \partial y, \partial Z / \partial x)$ . Moreover,  $K_s$  and  $K_n$  are the coefficients of longshore and cross-shore sand transport, respectively,  $K_2$  is the coefficient of the term given by Ozasa and Brampton (1980),  $\partial H / \partial s = \bar{e}_s \cdot \bar{\nabla} H$  is the longshore gradient of the wave height  $H$  measured parallel to the contour lines, and  $\tan \bar{\beta}$  is the characteristic slope of the breaker zone. In addition,  $C_0$  is the coefficient transforming the immersed weight expression into a volumetric expression ( $C_0 = 1 / \{(\rho_s - \rho)g(1 - p)\}$ ), where  $\rho$  is the density of seawater,  $\rho_s$  is the specific gravity of sand particles,  $p$  is the sand porosity, and  $g$  is the acceleration due to gravity).

The intensity of sand transport,  $P$ , in Eq. (1) is assumed to be proportional to the wave energy dissipation rate, as described by Serizawa et al. (2006), on the basis of the energetics approach of Bagnold (1963).  $P$  is determined by the wave energy dissipation rate due to wave breaking at a local point,  $\Phi_{\text{all}}$  (Eq. (2)), which can be determined from the calculation of the wave field.

$$P = \Phi_{\text{all}} \quad (2)$$

For the calculation of the wave field, the numerical simulation method of the energy balance equation given by Mase (2001), in which the directional spectrum of irregular waves is the variable to be solved, was employed with the additional term of energy dissipation due to wave breaking proposed by Dally et al. (1984). In this numerical simulation, the effects of wave refraction, wave breaking, and wave-sheltering by the sand spit itself are included.  $\Phi_{\text{all}}$  in Eq. (2), which defines the sum of the energy dissipation of each component wave due to breaking, was calculated from Eq. (3).

$$\Phi_{\text{all}} = f_D E = K \sqrt{g/h} [1 - (\Gamma/\gamma)^2] E \quad (f_D \geq 0) \quad (3)$$

Here,  $f_D$  is the energy dissipation rate,  $E$  is the wave energy,  $K$  is a coefficient expressing the intensity of wave dissipation due to breaking,  $h$  is the water depth,  $\Gamma$  is the ratio of the critical wave height to the water depth on a flat bottom, and  $\gamma$  is the ratio of the wave height to water depth,  $H/h$ . In addition, a lower limit was set for  $h$  in Eq. (3), similarly to in the work of Uda et al. (2014; 2016). The wave field was repeatedly calculated every 10 steps of the calculation of beach changes.

In the calculation of the wave field in the wave run-up zone, an imaginary depth was assumed, similarly to in Uda et al. (2014; 2016). Furthermore, the wave energy at locations with elevations higher than the berm height was set to 0. In the numerical simulation of beach changes, the sand transport and continuity equations ( $\partial Z / \partial t + \nabla \cdot \bar{q} = 0$ ) were solved on the  $x$ - $y$  plane by the explicit finite-difference method using a staggered mesh scheme.

When estimating the intensity of sand transport near the berm top and at the depth of closure, the intensity of sand transport was linearly reduced to 0 near the berm height and the depth of closure to prevent sand from being deposited in the zone higher than the berm height and to prevent the beach from being eroded in the zone deeper than the depth of closure, similarly to in the simulation by Uda et al. (2013). Further detail of the calculation method can be found in Uda et al. (2018).

### CALCULATION CONDITIONS

A model for predicting the formation of a compound recurved spit composed of many recurved sand spits similar to Graswarder spit was developed, assuming wave incidence from two opposing directions. By defining Cartesian coordinates  $(x, y)$ , a rectangular basin with lengths of 1.6 and 2.4 km in the  $x$ - and  $y$ -directions, respectively, was adopted as the calculation domain, as shown in Fig. 11. Since a sand spit is generally formed on a shallow sea, the water depth where the sand spit is formed was assumed to be 4 m. A sufficient volume of sand must be supplied from the upcoast boundary by longshore sand transport for a sand spit to be formed. When waves reach the coastline from the clockwise direction relative to the  $x$ -axis, longshore sand flows out of the left boundary, and it becomes difficult to handle the left boundary condition when the wave direction changes to counterclockwise in the next step. In this study, therefore, a high sand mound was placed in the calculation domain between  $x = -300$  and  $300$  m and between  $y = -1,200$  and  $-1,000$  m, so that a sufficient volume of sand for the elongation of a sand spit could be supplied to the coast. The initial shoreline configuration is given by a rectangle with a width of 300 m along the  $y$ -direction and a length of 600 m along the  $x$ -direction, as shown in Fig. 11.

When part of the sand mound with elevation higher than  $h_R$  is eroded, cross-shore sand movement due to the effect of gravity is forced to occur; this is caused by the falling of sand when the local slope exceeds the slope of the angle of repose of sand, as described in Serizawa et al. (2003). The crown height of the sand mound was assumed to be 51 m with a side slope of  $1/2$ , as schematically shown in Fig. 12, and the berm height and beach slope were assumed to be 1 m and  $1/20$ , respectively. Sand was only supplied from this sand mound, and longshore sand transport across the boundary was set to be 0.

A numerical simulation was carried out in two cases with a constant wave height of 1 m and wave period of 4 s. The wave direction  $\theta$  was defined as the angle relative to the  $x$ -axis. In Case 1, waves were incident periodically from two directions,  $45^\circ$  and  $-30^\circ$  relative to the  $x$ -axis, with a duration ratio of 0.85:0.15 while one cycle of the wave action from the two directions set to  $T = 5,000$  steps (2,500 hr), as schematically illustrated in Fig. 13. In Case 2, waves were incident from the two directions of  $45^\circ$  and  $-45^\circ$ . The mesh interval was 20 m and the time step was  $\Delta t = 0.5$  hr. The other calculation conditions are shown in Table 1.

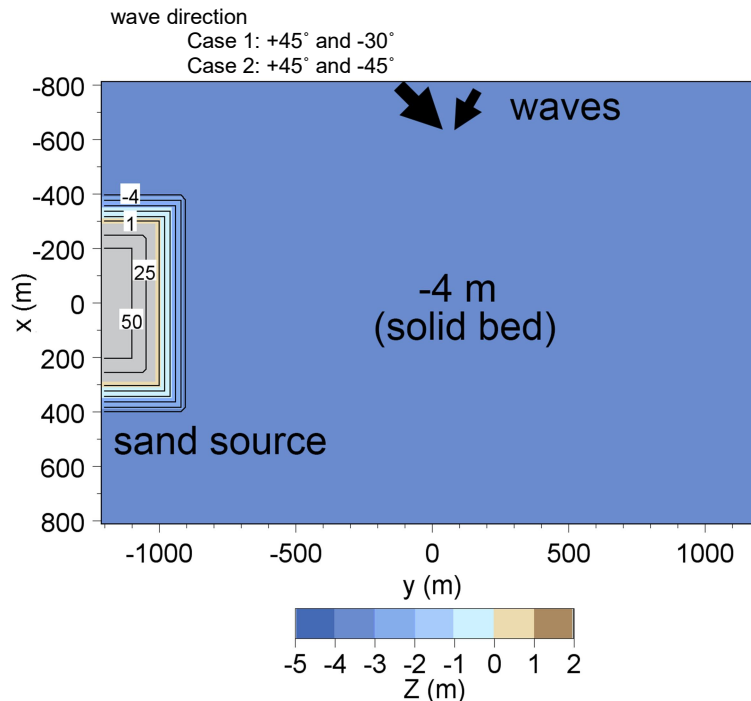


Figure 11. Initial bathymetry for numerical calculation of recurved sand spit.

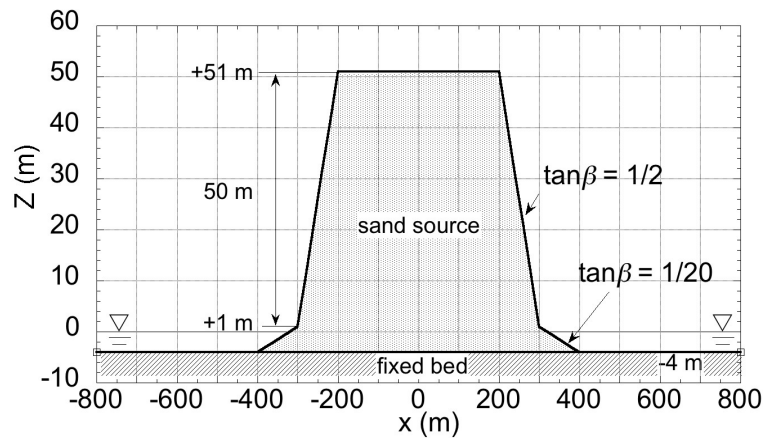


Figure 12. Crosssection of sand mound.

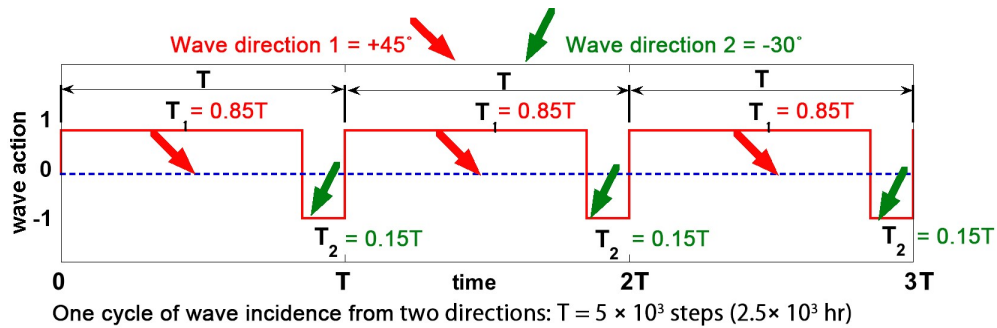


Figure 13. Schematic diagram of time change in wave incidence from two directions.

Table 1. Calculation conditions.	
Wave conditions	Incident waves: $H_i = 1$ m, $T = 4$ s, wave direction $\theta_i = 45^\circ$ and $-30^\circ$ (Case 1), $\theta_i = 45^\circ$ and $-45^\circ$ (Case 2) with a duration ratio of 0.85:0.15, Duration of one cycle: $2.5 \times 10^3$ hr ( $5 \times 10^3$ steps)
Berm height	$h_R = 1$ m
Depth of closure	$h_c = 4$ m
Equilibrium slope	$\tan \beta_e = 1/20$
Coefficients of sand transport	Coefficient of longshore sand transport $K_s = 0.2$ Coefficient of Ozasa and Brampton (1980) term $K_2 = 1.62K_s$ Coefficient of cross-shore sand transport $K_r = K_s$
Mesh size	$\Delta x = \Delta y = 20$ m
Time intervals	$\Delta t = 0.5$ hr
Duration of calculation	$2 \times 10^4$ hr ( $4 \times 10^4$ steps)
Boundary conditions	Shoreward and landward ends: $q_x = 0$ , right and left boundaries: $q_y = 0$
Calculation of wave field	Energy balance equation (Mase 2001) • Term of wave dissipation due to wave breaking: Dally et al. (1984) model • Wave spectrum of incident waves: directional wave spectrum density obtained by Goda (1985) • Total number of frequency components $N_f = 1$ and number of directional subdivisions $N_\theta = 8$ • Directional spreading parameter $S_{max} = 25$ • Coefficient of wave breaking $K = 0.17$ and $\Gamma = 0.3$ • Imaginary depth between minimum depth $h_0$ (0.5 m) and berm height $h_R$ • Wave energy = 0 where $Z \geq h_R$ • Lower limit of h in terms of wave decay due to breaking: 0.5 m

### CALCULATION RESULTS

Figure 14 shows the calculation results of the elongation of the recurved sand spit in Case 1, in which waves were incident periodically from the two directions of  $45^\circ$  and  $-30^\circ$  relative to the  $x$ -axis, up to  $4.0 \times 10^4$  steps. A recurved sand spit was formed under the condition that waves were incident from the direction of  $\theta = 45^\circ$  up to 4,250 steps and then from the direction of  $\theta = -30^\circ$  for the next 750 steps to form the initial recurved spit. The same procedure for the formation of a recurved spit was carried out repeatedly. The width of the sand spit gradually extended in the  $y$ -direction because of the longer duration of waves incident counterclockwise. Owing to the action of waves incident from

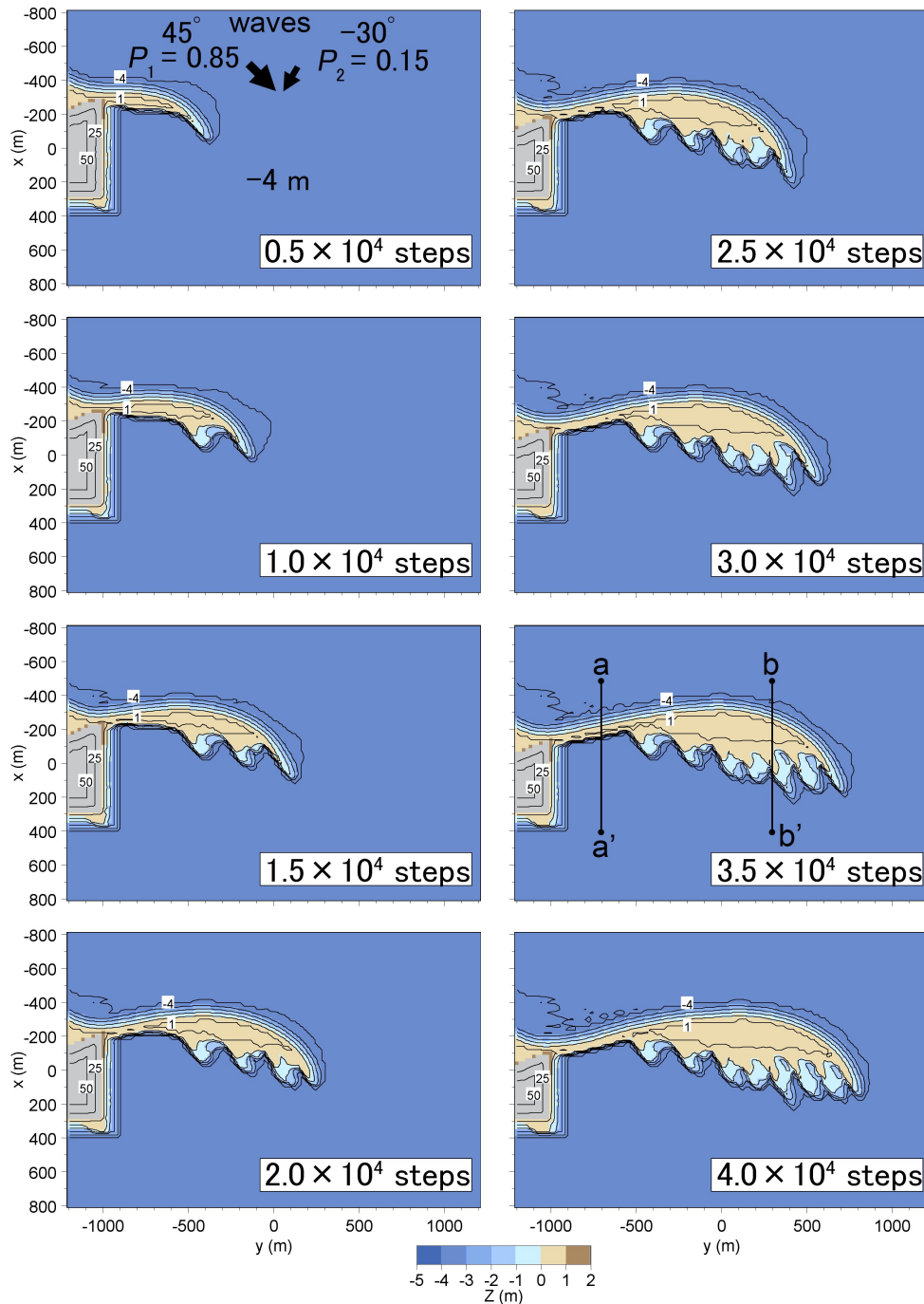


Figure 14. Predicted results of formation of recurved spit in Case 1, in which waves are incident periodically at angles of  $45^\circ$  and  $-30^\circ$ .

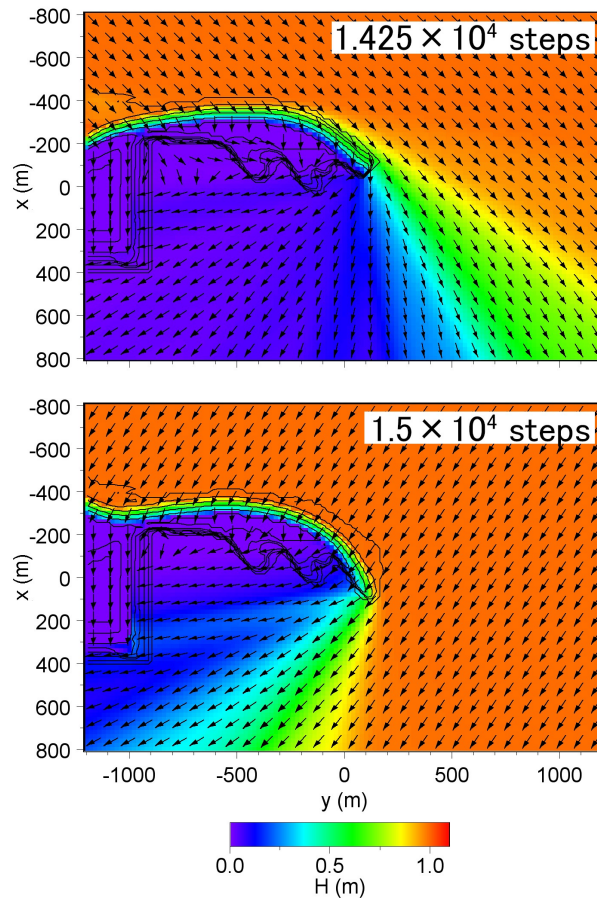


Figure 15. Wave fields after  $1.425 \times 10^4$  and  $1.5 \times 10^4$  steps in Case 1.

clockwise, the tip of the sand spit turned inward to form a recurved sand spit, and the size of the recurved spits gradually increased to the right. The number of recurved sand spits corresponds to the number of times that the wave direction changed from  $45^\circ$  to  $-30^\circ$ . The width of the recurved spit increased with the distance from the sand source along the  $y$ -direction in Case 1. The calculated results in Case 1 were similar to the sand spit in Namibia shown in Fig. 4.

Figure 15 shows the wave fields after  $1.425 \times 10^4$  and  $1.5 \times 10^4$  steps, after approximately three cycles of the wave action. When waves were incident from the counterclockwise direction relative to the sand spit, a wide wave-shelter zone was formed on the lee of the sand spit because of the larger wave angle. In contrast, when waves are incident from the clockwise direction, a narrow wave-shelter zone was formed.

Figure 16 shows the calculation results of the elongation of a recurved sand spit in Case 2, in which waves were incident periodically from the two directions of  $45^\circ$  and  $-45^\circ$  relative to the  $x$ -axis with a duration ratio of 0.85:0.15. A recurved sand spit was formed under the condition that waves were incident from the direction of  $\theta = 45^\circ$  up to 4,250 steps and then from the direction of  $\theta = -45^\circ$  for the next 750 steps to form the initial recurved spit. The same procedure for the formation of a recurved spit was carried out repeatedly.

A slender sand spit extended straight in Case 2 owing to the alternately changing oblique wave incidences of  $45^\circ$  and  $-45^\circ$  with a duration ratio of 0.85:0.15, because the rightward longshore sand transport is larger than the leftward transport owing to the longer duration of the waves obliquely incident at an angle of  $45^\circ$ . In this case, the sand spit maintained an approximately constant width, and the effect of the change in wave direction was only apparent near the tip of the sand spit. The shape of the sand spit resembles the Graswarder spit, as shown in Fig. 9, in terms of the extension of the recurved sand spit with a constant width.

Figure 17 shows the wave fields after  $1.425 \times 10^4$  and  $1.5 \times 10^4$  steps, after approximately three cycles of wave action. When waves were incident from the counterclockwise direction relative to the  $x$ -

axis, a wide wave-shelter zone was formed behind the recurved sand spit. In contrast, the size of the wave-shelter zone was significantly reduced when waves were incident from the clockwise direction, which may have caused longshore sand transport toward the  $-y$ -direction. It can be seen that the wave-sheltering effect plays an important role in the extension of a sand spit.

Figure 18 shows the shoreline configurations in Cases 1 and 2 after  $3.5 \times 10^4$  steps. The sand spit is straight in Case 2, whereas it is more recurved with increasing width in Case 1, and the overall shape becomes similar to that of an expanded bird wing. Figure 19 shows the change in the longitudinal profiles along  $y = -700$  m and  $300$  m in Cases 1 and 2, as shown by a-a' and b-b' in Fig. 18, respectively. The profiles along transect  $y = -700$  m in Cases 1 and 2 are approximately the same, although the location of the sand bar is slightly closer to the  $x$ -axis in Case 2. Along transect  $y = 300$  m, the location of the sand bar is markedly landward in Case 1 compared with that in Case 2.

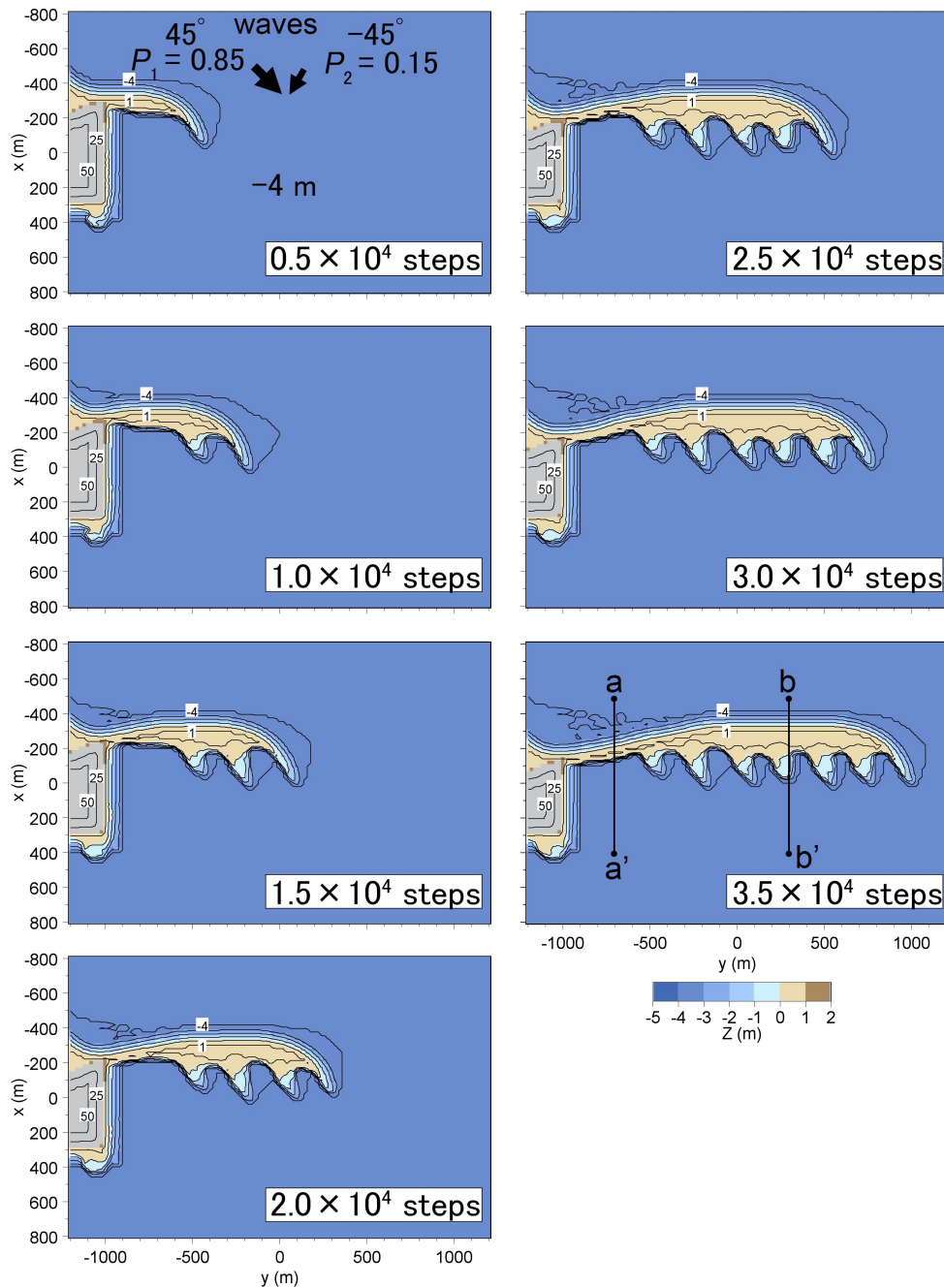


Figure 16. Predicted results of formation of recurved spit in Case 1, in which waves are incident periodically at angles of  $45^\circ$  and  $-45^\circ$ .

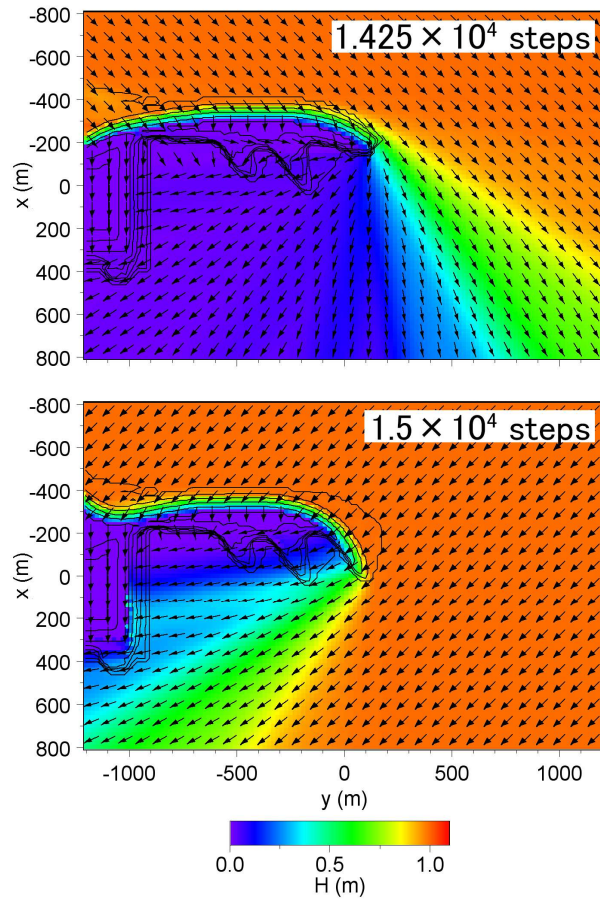


Figure 17. Wave fields after  $1.425 \times 10^4$  and  $1.5 \times 10^4$  steps in Case 2.

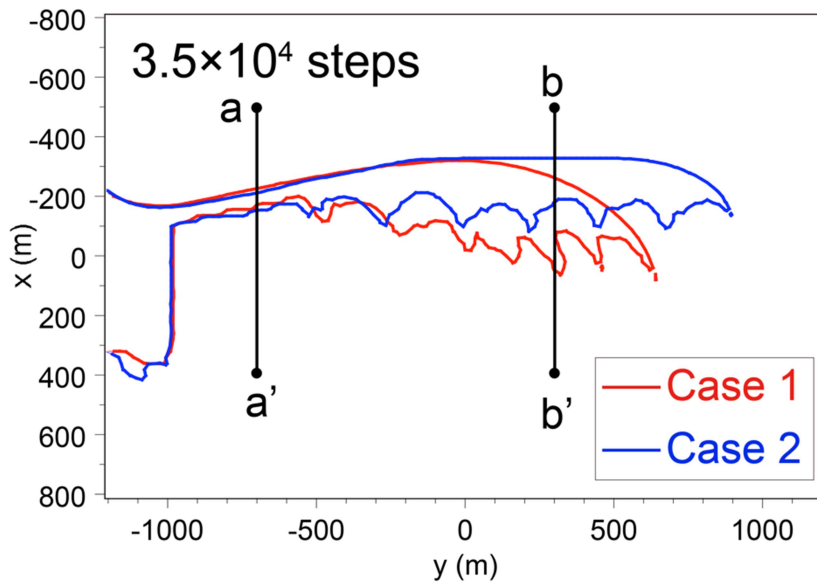


Figure 18. Shoreline configurations in Cases 1 and 2.

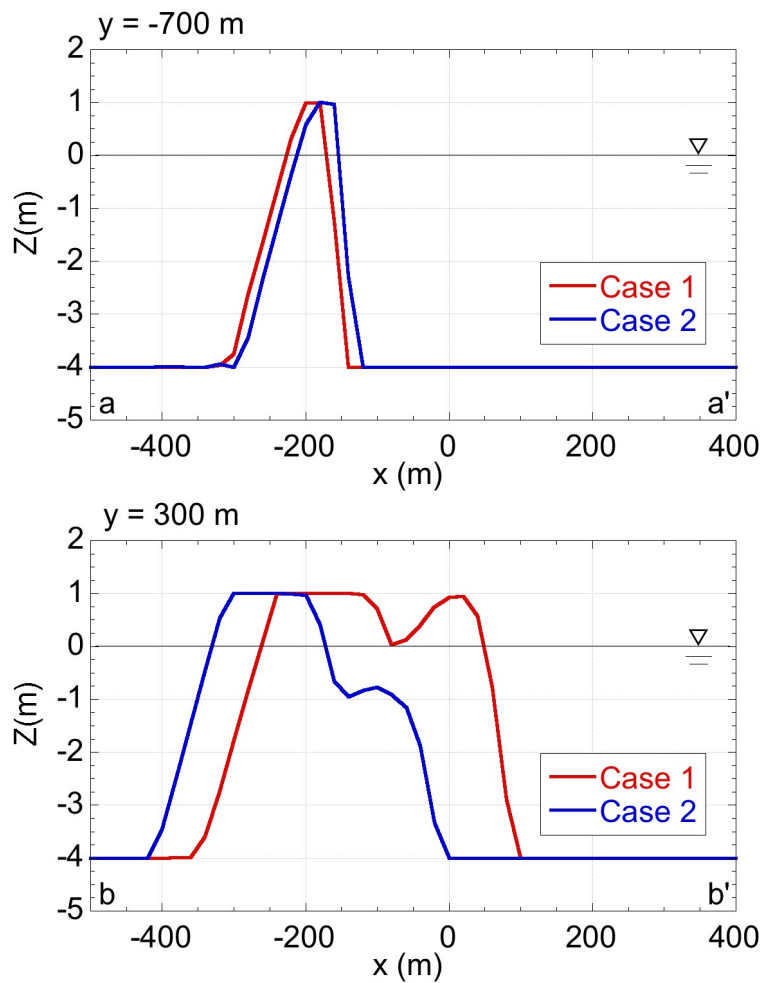


Figure 19. Longitudinal profiles along transects  $y = -700$  m and  $300$  m in Cases 1 and 2.

## CONCLUSIONS

Taking the recurved sand spits in Namibia, Sandy Hook on the US east coast, and Graswarder spit in Germany as examples, the morphological features of recurved sand spits were studied. The sand spits in Namibia and Sandy Hook were classified as typical recurved sand spits; the shoreline of a recurved sand spit extends such that the elongating tip is smoothly connected to the elongation direction of the overall sand spit. However, in Graswarder spit, the previous shoreline intersected at an acute angle with the overall extending direction of the sand spit, in contrast to the other two cases. In this study, the elongation of a compound spit with many recurved spits superimposed on each other, as in Graswarder spit, was predicted using the BG model. It was confirmed that when two sets of waves arrive from different directions, such a recurved (compound) sand spit can be formed. The measured and calculated characteristics were in good agreement.

## REFERENCES

- Ashton, A., A.B. Murray, and O. Arnault. 2001. Formation of coastline features by large-scale instabilities induced by high angle waves, *Nature*, 414, 296-300.
- Bagnold, R.A. 1963. *Mechanics of marine sedimentation*, Hill, M.N. ed. In *The Sea*, Vol. 3, Wiley, New York, 507-528.
- Bird, Eric. 2008. *Coastal Geomorphology, An Introduction*, Second Edition, John Wiley & Sons, Ltd.
- Bird, E.C.F. 2010. *Encyclopedia of the World's Coastal Landforms*, Volume I, Dordrecht; Heidelberg, Springer, 641-644.
- British Maritime Technology, Ltd. 1986. *Global Wave Statistics*, Teddington Middlesex, UK.

- Dally, W.R., R.G. Dean, and R.A. Dalrymple. 1984. A model for breaker decay on beaches, *Proceedings 19<sup>th</sup> International Conference on Coastal Engineering*, ASCE, 82-97.
- Goda, Y. 1985. *Random Seas and Design of Maritime Structures*, University of Tokyo Press, Tokyo, p. 323.
- Mase, H. 2001. Multidirectional random wave transformation model based on energy balance equation, *Coastal Eng. J.*, JSCE, 43(4), 317-337.
- Ozasa, H., and A.H. Brampton. 1980. Model for predicting the shoreline evolution of beaches backed by seawalls, *Coastal Eng.*, 4, 47-64.
- Serizawa, M., T. Uda, T. San-nami, and K. Furuike. 2003. Prediction of depth changes on *x-y* meshes by expanding of contour-line change model, *Ann. J. Coastal Eng.*, JSCE, 50, 476-480. (in Japanese)
- Serizawa, M., T. Uda, T. San-nami, and K. Furuike. 2006. Three-dimensional model for predicting beach changes based on Bagnold's concept, *Proceedings of 30<sup>th</sup> International Conference on Coastal Engineering*, ASCE, 3155-3167.
- Uda, T., M. Gibo, T. Ishikawa, S. Miyahara, T. San-nami, and M. Serizawa. 2013. Change in carbonate beach triggered by construction of a bridge on Irabu Island and its simulation using BG model, *Asian and Pacific Coasts 2013, Proceedings of 7<sup>th</sup> International Conference*, 24-32.
- Uda, T., M. Serizawa, and S. Miyahara. 2014. Development of sand spits and cusped forelands with rhythmic shapes and their deformation by effects of construction of coastal structures (Chap. 19), 419-450, in 'Computational and Numerical Simulations' Awrejcewicz, L. ed., INTEC.
- Uda, T., M. Serizawa, and S. Miyahara. 2016. Formation of cusped foreland in field subject to wave-sheltering effect of islands, *Proceedings of 35<sup>th</sup> International Conference on Coastal Engineering*, ASCE, sediment.4, 1-14.
- Uda, T., M. Serizawa, and S. Miyahara. 2018. *Morphodynamic model for predicting beach changes based on Bagnold's concept and its applications*, INTEC, London, UK.  
Doi: <http://dx.doi.org/10.5772/intechopen.81411>
- Zenkovich, V. P. 1967. *Processes of Coastal Development*, Interscience Publishers, Div. of John Wiley and Sons, ING, New York, p. 751.